Molecular Microbiology (2005) **55**(5), 1346–1356 doi:10.1111/j.1365-2958.2005.04477.x

Two substrate-targeting sites in the *Yersinia* protein tyrosine phosphatase co-operate to promote bacterial virulence

Maya I. Ivanov,[1] Jeanne A. Stuckey,[2†] Heidi L. Schubert,[2‡] Mark A. Saper[2*] and James B. Bliska[1*]

[1]*Department of Molecular Genetics and Microbiology and Center for Infectious Diseases, State University of New York at Stony Brook, Stony Brook, NY 11794-5222, USA.*
[2]*Department of Biological Chemistry and Biophysics Research Division, University of Michigan, Ann Arbor, MI 48109-1055, USA.*

Summary

YopH is a protein tyrosine phosphatase and an essential virulence determinant of the pathogenic bacterium *Yersinia*. *Yersinia* delivers YopH into infected host cells using a type III secretion mechanism. YopH dephosphorylates several focal adhesion proteins including p130Cas in human epithelial cells, resulting in disruption of focal adhesions and cell detachment from the extracellular matrix. How the C-terminal protein tyrosine phosphatase domain of YopH targets specific substrates such as p130Cas in the complex milieu of the host cell has not been fully elucidated. An N-terminal non-catalytic domain of YopH binds p130Cas in a phosphotyrosine-dependent manner and functions as a novel substrate-targeting site. The structure of the YopH protein tyrosine phosphatase domain bound to a model phosphopeptide substrate was solved and the resulting structure revealed a second substrate-targeting site ('site 2') within the catalytic domain. Site 2 binds to p130Cas in a phosphotyrosine-dependent manner, and co-operates with the N-terminal domain ('site 1') to promote efficient recognition of p130Cas by YopH in epithelial cells. The identification of two substrate-targeting sites in YopH that co-operate to promote epithelial cell detachment and bacterial virulence reinforces the importance of protein–protein interactions for determining protein tyrosine phosphatase specificity *in vivo*, and highlights the sophisticated nature of microbial pathogenicity factors.

Accepted 10 November, 2004. *For correspondence. E-mail jbliska@ms.cc.sunysb.edu; Tel. (+1) 631 632 8782; Fax (+1) 631 632 4294; and E-mail saper@umich.edu; Tel. (+1) 734 764 3353; Fax (+1) 734 764 3323. Present addresses: †Life Sciences Institute, University of Michigan, Ann Arbor, MI 48109-2216, USA; ‡Department of Biochemistry, University of Utah, Salt Lake City, UT 84132, USA.

© 2005 Blackwell Publishing Ltd

Introduction

Yersinia pestis, *Yersinia pseudotuberculosis* and *Yersinia enterocolitica* are Gram-negative bacterial pathogens of humans and a variety of animal species. *Y. pestis* is the agent of plague (Perry and Fetherston, 1997). *Y. pseudotuberculosis* and *Y. enterocolitica* cause enteritis and mesenteric lymphadenitis (Carniel *et al.*, 2002). The human-pathogenic *Yersinia* species share a number of common virulence factors (Revell and Miller, 2001; Carniel, 2002). One such virulence determinant is a type III secretion system (TTSS) encoded on a 70 kb plasmid (Cornelis, 2002; Ramamurthi and Schneewind, 2002). The *Yersinia* TTSS is homologous to TTSSs found in a variety of other bacterial pathogens (Hueck, 1998). The *Yersinia* TTSS exports a set of proteins (Yops and LcrV) upon contact with host cells (Cornelis, 2002; Ramamurthi and Schneewind, 2002). These proteins are released into extracellular milieu, inserted into the host cell membrane or delivered into the cytoplasm of the host cell (Cornelis, 2002; Ramamurthi and Schneewind, 2002). The Yops and LcrV act in concert to thwart innate cellular immune responses to *Yersinia* (Cornelis, 2002; Ramamurthi and Schneewind, 2002).

YopH is a protein tyrosine phosphatase (PTP) that is delivered into the cytoplasm of host cells infected by *Yersinia* (Guan and Dixon, 1990; Bliska *et al.*, 1991). YopH has been shown to uncouple multiple signal transduction pathways in host cells (Fällman *et al.*, 1997; Bliska, 2000). In human epithelial cells YopH dephosphorylates several focal adhesion proteins, including p130Cas (Cas) (Black and Bliska, 1997; Persson *et al.*, 1997). Dephosphorylation of Cas and other focal adhesion proteins by YopH results in cellular retraction from the extracellular matrix and inhibition of integrin-mediated bacterial invasion (Black and Bliska, 1997; Persson *et al.*, 1997).

The 468-amino-acid YopH protein is composed of two modular domains linked by a proline-rich sequence. The PTP domain is comprised of residues ≈163–468 (Zhang *et al.*, 1992). The three-dimensional structure of the PTP

domain has been determined (Stuckey *et al*., 1994). Residues 403–410 form a phosphate-binding loop (P-loop) within the active site. Substitution of the essential catalytic Cys residue at position 403 to Ser results in a catalytically inactive enzyme that retains the ability to bind substrates at the active site (substrate trapping) (Guan and Dixon, 1990; Bliska *et al*., 1991; Montagna *et al*., 2001). Substitution of the essential catalytic Arg residue at position 409 with Ala ablates substrate binding and catalysis by YopH (Guan and Dixon, 1990; Zhang *et al*., 1994a; Montagna *et al*., 2001). Residues 1–129 of YopH comprise an N-terminal domain, which contains signals required for TTSS-mediated delivery of YopH into host cells (Cornelis, 2002). The N-terminal region also binds to tyrosine-phosphorylated proteins and functions within the host cell as a substrate-targeting domain (Black *et al*., 1998; Deleuil *et al*., 2003). Several residues within the N-terminal domain that are required for substrate targeting (e.g. Val31) were identified using a genetic approach (Montagna *et al*., 2001). Three-dimensional structures have been determined for the N-terminal domain using X-ray crystallography (Smith *et al*., 2001) or NMR (Khandelwal *et al*., 2002). The fold of the N-terminal domain is unlike that of SH2 or PTB domains. This region of YopH appears to represent a novel type of phosphotyrosine-binding domain (Smith *et al*., 2001).

Previous studies revealed that YopH binds to the prototypical substrate Cas *in vivo* via either the N-terminal domain (hereafter referred to as 'site 1') or the active site (hereafter referred to as 'A site') containing the substrate-trapping C403S mutation (Black *et al*., 1998; Montagna *et al*., 2001). However, inactivation of substrate-binding activity in site 1 using the V31G mutation and in the A site using the R409A mutation did not eliminate interaction with Cas (Montagna *et al*., 2001) (see Fig. 3), suggesting that another substrate binding site may be present in YopH. This possibility was investigated.

Results

Persson *et al*. (1999) have implicated an exposed loop in the catalytic domain of YopH (residues 223–226) as being important for efficient focal contact targeting. To determine whether residues 223–226 of YopH could be important for interaction with Cas, these residues were deleted ('Δ' mutation) in the context of the A site mutant protein ($YopH^{R409A}$). HeLa cells were infected with *Y. pseudotuberculosis* strains producing $YopH^{R409A}$ or the double mutant $YopH^{\Delta RA}$, and immunofluorescence microscopy was used to detect localization of YopH to focal adhesions. As shown in Fig. 1, $YopH^{R409A}$ and $YopH^{\Delta RA}$ showed equivalent focal adhesion localization activity (compare Fig. 1B and D). To confirm these results, the infected cells were lysed and an interaction of Cas with YopH was assayed by immunoprecipitation and anti-pTyr immunoblotting. A similar amount of pTyr-containing protein p130 (corresponding to Cas) was co-precipitated with $YopH^{R409A}$ and $YopH^{\Delta RA}$ (Fig. 1E and F, lanes 3 and 5), indicating that residues 223–226 of YopH are dispensable for interaction with Cas.

We have determined the crystal structure, refined to 3.0 Å resolution, of an inactive YopH catalytic domain (residues 163–468) with Ser substituted for the active site Cys403 ($YopH^{C403S}$) bound to the phosphopeptide substrate DADEpYL, which is based on an autophosphorylation site of the EGFR (Zhang *et al*., 1994b). We have also determined the 2.5 Å resolution structure of the wild-type YopH complexed with the same peptide but containing difluorophosphonomethyl-phenylalanine, a non-hydrolysable analogue of phosphotyrosine (DADEdfpYL). The two crystals are isomorphous and each contains two enzyme complexes in a *P*1 unit cell. Details of the crystals and structure solution are shown in Table 1. While this manuscript was in preparation, Phan *et al*. (2003) reported the structure of the catalytic domain of YopH in complex with a non-hydrolysable hexapeptide substrate.

Both crystal structures reported here show well-ordered electron density consistent with a bound peptide at a second substrate binding site (hereafter referred to as 'site 2'), approximately 38 Å from the active site P-loop and about 35 Å from the putative focal complex targeting loop comprised of residues 223–226 (Fig. 2A). The structure reported by Phan *et al*. (2003) also contains a peptide bound to site 2. These authors suggested that site 2 could be involved in substrate recognition *in vivo*, although no functional data in support of this idea were obtained (Phan *et al*., 2003). The electron density at site 2 clearly defines at least five of the six peptide side-chain positions (Fig. 2B). In contrast, peptide electron density at the active site of the difluorophosphonate structure clearly shows only three to four of the side-chains, and only the phosphotyrosine is resolved at the active site in the $YopH^{C403S}$ structure (data not shown). The better density at site 2 may be indicative of a tighter affinity than the active site or it may result from an arginine from another molecule in the unit cell (data not shown) that makes hydrogen bonds to the phosphotyrosine.

As shown in Fig. 2A, the DADEdfpYL phosphopeptide at site 2 binds in a groove formed by residues at the end of helix α4, the beginning of β-strand β6 and the loop between α2 and β3 (secondary structure designations are from Stuckey *et al*., 1994). The conformation of the peptide main-chain is similar to two consecutive β-turns. Most of the specific interactions are to the phosphotyrosine residue, which lies parallel to the protein surface, rather than buried in a deep pocket as it is in the active site. Two charged residues ligate the phosphonate (Fig. 2C): Arg278, from the α2–β3 loop, forms a bidentate salt-

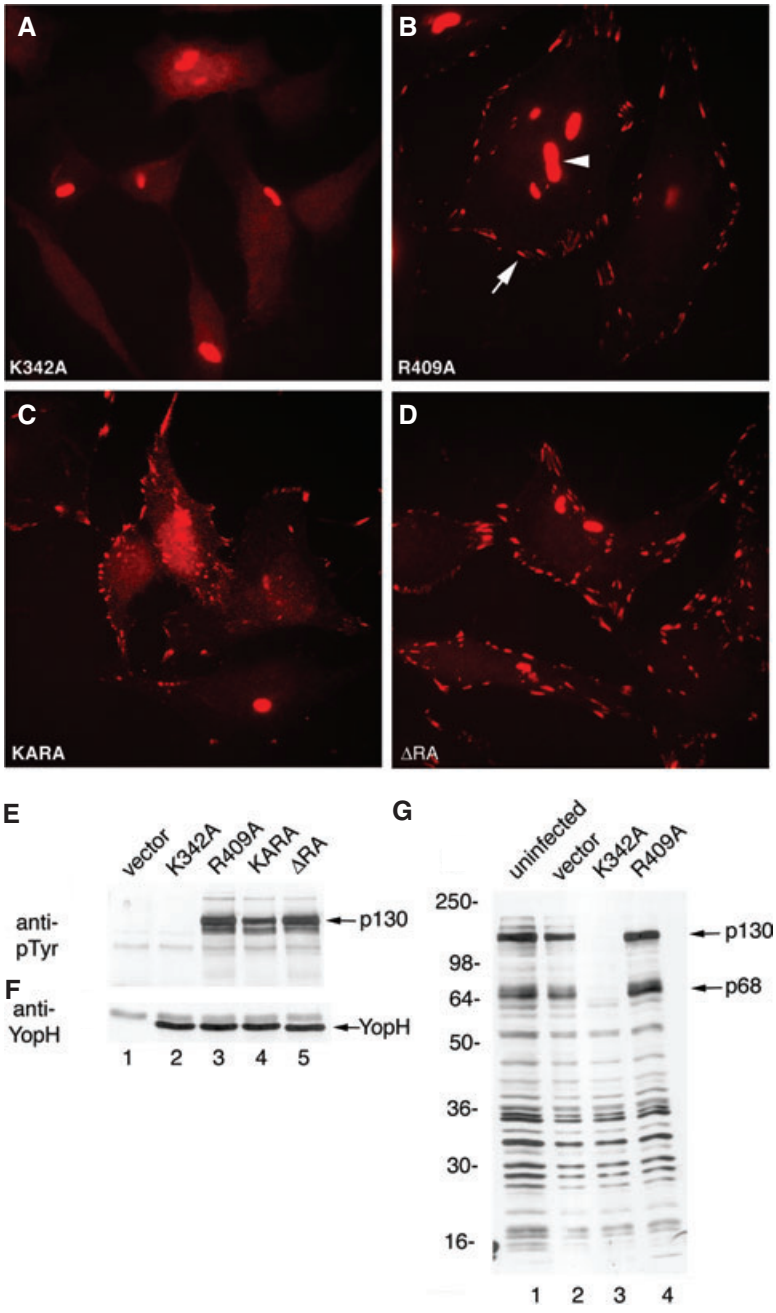

Fig. 1. Site 2 in YopH is important for substrate binding in host cells. HeLa cells were infected with *Y. pseudotuberculosis* for 2 h. The strains used carried an empty vector (vector), and therefore expressed no YopH, or carried vectors expressing YopH^{K342A}M45 (K342A), YopH^{R409A}M45 (R409A), YopH^{K342AR409A}M45 (KARA) or YopH$^{\Delta R409A}$M45 (ΔRA).
A–D. Subcellular localization of mutant YopH proteins was examined by immunofluorescence microscopy using a monoclonal antibody specific to the M45 epitope appended to each of the mutant YopH proteins. Arrows point to focal adhesions, and arrowheads point to infecting bacteria that also stain with the antibody.
E and F. Binding of Cas (p130) to mutant YopH proteins was examined by co-immunoprecipitation and immunoblotting. Mutant YopH proteins were immunoprecipitated from lysates of the infected cells using anti-M45. Immunoblots were developed with anti-M45 to control for YopH recovery (F) or anti-pTyr antibodies to detect Cas (p130) (E).
G. Lysates of uninfected or cells infected for 2 h were analysed by immunoblotting with anti-pTyr to detect dephosphorylation of Cas (p130) and paxillin (p68). Positions of molecular weight standards are shown on the left.

bridge with the phosphate similar to what is observed with the catalytic Arg in the active site. Lys342 forms a salt-bridge to the phosphonate oxygens as well as one fluorine atom and Glu4 (P−1 position) of the peptide. Two Ser residues also make hydrogen bonds to the phosphonate oxygens. Lys386 forms a hydrogen bond with the Glu4 carbonyl and non-polar contacts with the phosphonate ring. Other peptide main-chain atoms also make hydrogen bonds with the protein (Fig. 2C). The specific interactions with the phosphonate suggest that pTyr is probably the primary determinant of specificity for peptides binding to this site. As there are few other specific interactions with the other side-chains (except for Glu4), this binding site may accommodate a variety of pTyr-containing sequences such as those observed in the multiple phosphorylation motifs present in the Cas natural substrate.

To determine whether site 2 is important for interaction of YopH with Cas *in vivo*, we introduced a Lys342 to Ala (K342A) mutation into the YopH^{R409A} protein to inactivate site 2. The resulting YopH protein mutated in site 2 and the P-loop (YopH^{KARA}) showed reduced localization to focal adhesions, and increased protein localization to the

Table 1. Diffraction and refinement statistics for YopH–peptide complexes.

	$YopH^{C403S}$ (163–468) + Ac-DADE(pY)L-NH_2	YopH (163–468) + Ac-DADE(dfpY)L-NH_2
Space group	*P*1	*P*1
Cell dimensions (Å)		
a	54.5	54.13
b	48.4	47.17
c	71.9	71.82
α	111.9	104.45
β	110.1	115.05
γ	90.3	90.00
Resolution (Å)	20–3.0	50–2.5
Number of reflections	10084	18319
R_{merge}	0.118	0.075
Completeness (%)	86	85.5
Number of protein molecules	2	2
Protein residues	182–468 (A) 186–468 (B)	187–468 (A) 187–468 (B)
Peptide residues (molecule, site)	1 (A, active) 5 (A, site 2) 1 (B, active) 5 (B, site 2)	4 (A, active) 6 (A, site 2) 4 (B, active) 6 (B, site 2)
Total number of atoms	4588	4831
Number of waters	89	297
R_{work}/R_{free}	0.181/0.249	0.178/0.229
rmsd bonds (Å)	0.008	0. 007
rmsd angles (°)	1.18	1.18

pY, phosphotyrosine; dfpY, difluorophosphonomethyl-phenylalanine; rmsd, root mean square deviation.

cytosol of the infected cells (compare Fig. 1B and C). In addition, co-precipitation of Cas with $YopH^{KARA}$ in infected cells was reduced as compared with the controls (Fig. 1E and F, lane 4). These results suggest that site 2 is involved in targeting YopH to Cas *in vivo*. The K342A mutation is not expected to diminish the intrinsic catalytic activity of YopH, as it is distant from the A site. To confirm that the K342A mutation does not inhibit intrinsic catalytic activity, HeLa cells were infected with a *Y. pseudotuberculosis* strain producing $YopH^{K342A}$, which is only mutated in site 2. Dephosphorylation of total cellular proteins after a 2 h infection was examined by anti-pTyr immunoblotting. As shown in Fig. 1G, bands of 130 kDa (p130) and 68 kDa (p68) were dephosphorylated in the presence of $YopH^{K342A}$. These bands have previously been shown to correspond to Cas and paxillin respectively (Black and Bliska, 1997; Black *et al*., 1998). Further evidence that $YopH^{K342A}$ did not have diminished catalytic activity was shown by immunofluorescence microscopy and immunoprecipitation. $YopH^{K342A}$ did not localize to focal adhesions (Fig. 1A), and did not co-precipitate with Cas (Fig. 1E and F, lane 2).

To determine whether sites 1 and 2 can function independently to bind substrate, mutations designed to inactivate site 1, or site 1 and site 2, were introduced into the A site mutant $YopH^{R409A}$. After HeLa cells were infected with *Y. pseudotuberculosis* strains producing these proteins, substrate-binding activity was measured using immunofluorecence microscopy and immunoprecipitation. As shown above, inactivation of site 2 and the A site ($YopH^{KARA}$) reduced, but did not eliminate, focal adhesion localization (Fig. 3B) or Cas binding (Fig. 3D–F, lane 5). Inactivation of site 1 and the A site ($YopH^{VGRA}$) eliminated focal adhesion localization activity (Fig. 3A) and diminished, but did not eliminate, interaction of YopH with Cas (Fig. 3D–F, lane 3). Inactivation of site 1, site 2 and the A site ($YopH^{VGKARA}$) further reduced the ability of YopH to bind Cas (Fig. 3D–F, lane 4). Densitometry was used to measure the signal intensities of the Cas bands detected in Fig. 3E, and these signals were normalized to the amounts of Cas present in lysates before immunoprecipitation (Fig. 3G). The calculations show that inactivation of site 2 decreased Cas binding by approximately twofold in the context of an intact site 1 ($YopH^{RA}$ versus $YopH^{KARA}$) and by ≈24-fold in the context of a mutated site 1 ($YopH^{VGRA}$ versus $YopH^{VGKARA}$). These results show that sites 1 and 2 can function independently to bind Cas in host cells (Fig. 3H). Of the two, site 1 appears to bind more avidly to Cas, which may explain why site 1 is sufficient for focal adhesion localization.

To confirm that site 2 binds Cas directly, we carried out an *in vitro* binding reaction with purified proteins. Purified Cas protein was phosphorylated using the Src kinase. As shown in Fig. 4A, phosphorylation of Cas (p-Cas) was evident by a decreased mobility during SDS-PAGE, and increased reactivity with anti-pTyr antibody. The catalytic domains (CDs; residues 172–468) of YopH proteins with mutations in A site or site 2, or both, were purified as GST

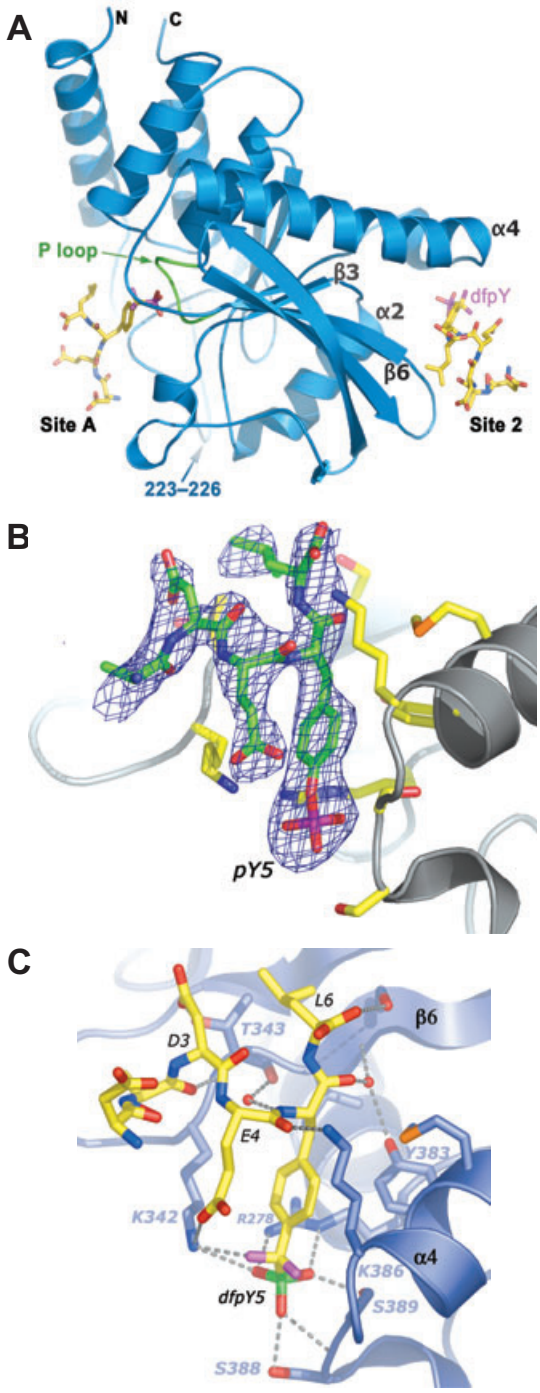

Fig. 2. Crystal structures of YopH catalytic domain complexed with phosphotyrosine (pY)- or phosphonodifluoromethyl-phenylalanine (dfpY)-containing peptides.
A. Cartoon representation of the dfpY-containing peptide complex showing location of peptides bound to the active site P-loop (A site) and site 2. The location of the putative focal complex targeting loop, residues 223–226, is also shown.
B. Simulated annealing F_{obs}–F_{calc} omit electron density of the bound pY-containing peptide at site 2. Density is well resolved for residues 2–6.
C. Close-up of the dfpY peptide (yellow) at site 2 showing potential hydrogen bonds with the protein structure (blue).
The figure was prepared with MacPyMOL (DeLano Scientific).

fusion constructs (GST–YopHCD). GST fusion proteins were bound to beads, incubated with p-Cas, and after washing, the amount of p-Cas bound to the GST fusion proteins was measured by anti-Cas immunoblotting. The highest level of binding to full-length Cas and several Cas truncation products was observed with the positive control YopHCD^{C403S} construct (Fig. 4B, lane 2). Mutation of the catalytic Cys residue at position 403 to Ser results in trapping of substrates at the active site (Guan and Dixon, 1990; Bliska *et al.*, 1991; Montagna *et al.*, 2001). Reduced Cas-binding activity was observed when 10-fold less YopHCD^{C403S} was bound to the beads (lane 1). In addition, when YopHCD^{R409A} and YopHCD^{KARA} were used in binding reactions, less Cas bound to the latter construct, indicating that site 2 binds directly to tyrosine-phosphorylated Cas (compare lanes 3 and 4).

To evaluate the importance of sites 1 and 2 for the biological activity of YopH, HeLa cells were infected with *Y. pseudotuberculosis* strains producing catalytically active YopH proteins with mutations in site 1, site 2 or both. Rounding and detachment of the HeLa cells in response to disruption of focal adhesions by YopH activity was measured by phase contrast microscopy, and by a quantitative viable cell assay (MTT assay). As shown in Fig. 5, wild-type YopH caused ≈80% of the HeLa cells to detach (Fig. 5B and G), while the catalytically inactive YopH^{R409A} protein did not cause any detachment (Fig. 5C and G). Approximately 60% of the cells detached when site 1 (YopH^{V31G}) or site 2 (YopH^{K342A}) were inactivated, while fewer cells detached (≈40%) when both sites were inactivated (YopH^{VGKA}) (Fig. 5D–G). Therefore, sites 1 and 2 cooperate to promote cell detachment by YopH in an *in vitro* infection assay.

A mouse infection assay (Bliska *et al.*, 1991) was used to evaluate the importance of site 1 and site 2 for the virulence function of YopH. *Y. pseudotuberculosis* is highly lethal for mice via the intravenous route of infection; this infection model approximates the systemic phase of plague (Une and Brubaker, 1984). Mice were infected with an equal mixture of a test strain and a chloramphenicol-resistant *yopH::cam* null mutant as a reference strain. The ability of mutant test strains to out-compete the reference strain for colonization of the spleen was determined by a competitive index (CI) assay. Test strains contained mutant *yopH* alleles introduced into the native location on the virulence plasmid. A test strain used as a wild-type control was constructed by introducing a silent mutation resulting in an Nde restriction site at the *yopH* initiation codon (*yopH*^{Nde}). As shown in Fig. 6, the wild-type test strain (*yopH*^{Nde}) out-competed the reference strain by a factor of ≈100 (geometric mean of control CI = 0.015). In contrast, the test strain expressing catalytically inactive YopH (*yopH*^{R409A}) did not out-compete the reference strain (geometric mean CI = 2.54). Test strains mutated in the

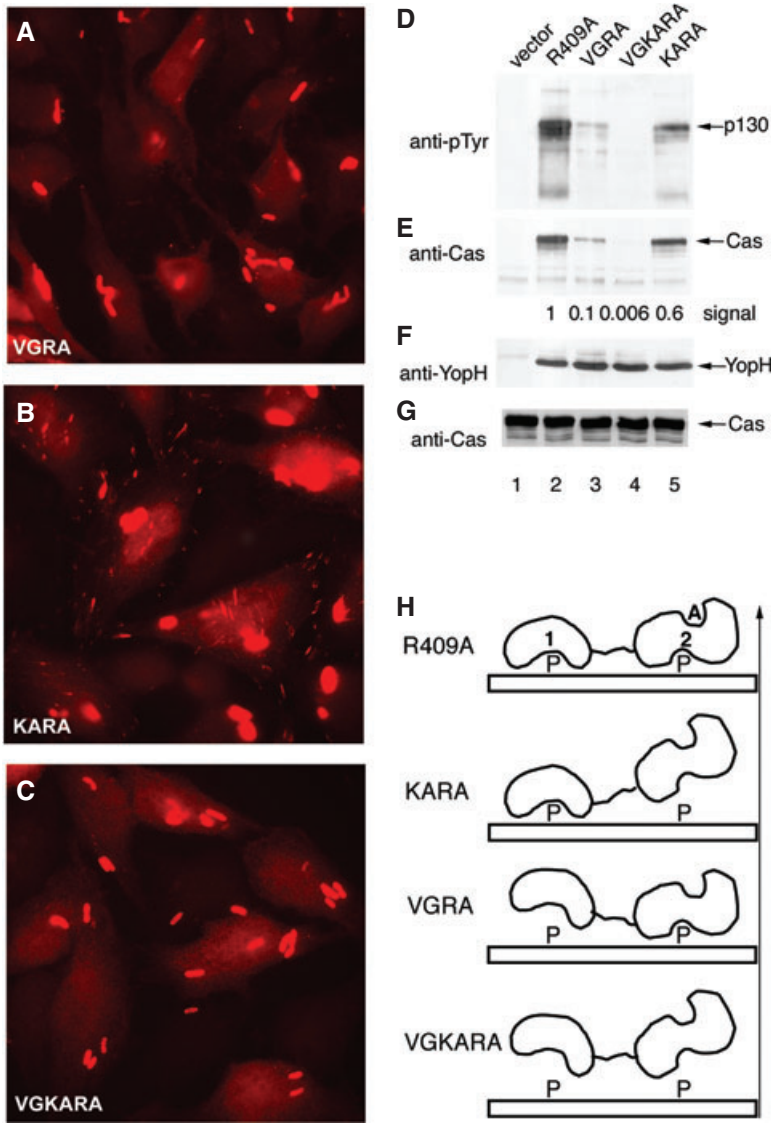

Fig. 3. Sites 1 and 2 can function independently to bind Cas in host cells. HeLa cells were infected and processed as in the legend to Fig. 1. The *Y. pseudotuberculosis* strains expressed no YopH (vector), YopH^{V31GR409A}M45 (VGRA), YopH^{V31GK342A409A}M45 (VGKARA), YopH^{K342AR409A}M45 (KARA) or YopH^{R409A}M45 (R409A).
A–C. Subcellular location of mutant YopH proteins as determined by immunofluorescence microscopy.
D–F. Co-immunoprecipitation of Cas with mutant YopH proteins was examined by immunoblotting with anti-pTyr, anti-Cas or anti-M45 antibodies.
G. Samples of infected cell lysates that were used for immunoprecipitations were analysed by immunoblotting with anti-Cas antibodies. Densitometry was used to measure the signal intensities of the Cas bands in lanes 2–5 of (E) and (G). Signal intensities of immunoprecipitated Cas bands (E) were normalized to the signal intensities of the Cas bands in the lysates (G). The signal intensity of the Cas band in lane 2 of (E) is assigned an arbitrary value of 1. The corresponding signal intensities of the other bands are indicated below (E) (signal).
H. Model depicting YopH interacting with a multiply phosphorylated (P) substrate through sites 1 and 2. The active site (A) is represented in a non-substrate-trapping form (R409A mutant). Mutant proteins are depicted in order of increasing substrate binding strength (from bottom to top, following direction of arrow).

focal contact targeting loop (*yopH*$^{\Delta 223-226}$), in site 2 (*yopH*^{K342A}) or in site 1 (*yopH*^{V31G}), had geometric mean CI values of 0.011, 0.014 and 0.023, respectively, and the CI data for these competitions were not significantly different (unpaired Student's *t*-test) from the control competition. The competition data for the test strain mutated in sites 1 and 2 (*yopH*^{VGKA}) (geometric mean CI = 0.033) was significantly different ($P = 0.044$) from the control competition (Fig. 6). Therefore, sites 1 and site 2 in YopH co-operate to promote substrate targeting *in vivo*, and this activity is important for *Yersinia* virulence.

Discussion

It is well established that targeting domains play a key role in substrate recognition by PTPs (Mauro and Dixon, 1994; Tonks and Neel, 2001). As shown here, substrate recognition by YopH involves two substrate-targeting sites that function in a cooperative manner. Other PTPs, such as SHP-2, contain duplicate substrate-targeting domains in the form of tandem SH2 domains (Tonks and Neel, 2001). In the case of SHP-2, the phosphotyrosine residues recognized by the SH2 domains serve as docking sites for the enzyme, but are not dephosphorylated by the catalytic domain. In contrast, the phosphotyrosine residues that are recognized by sites 1 and 2 in YopH may serve as docking sites initially, but are ultimately dephosphorylated by the catalytic domain. The substrate region of Cas contains multiple phosphorylation sites that are on average 21 residues apart (Bouton *et al.*, 2001). It is likely that sites 1 and 2 allow YopH to act in a highly processive manner to dephosphorylate the substrate region of Cas. However, the finding that site 2 is on the opposite side of the catalytic domain from the A site makes it unlikely that

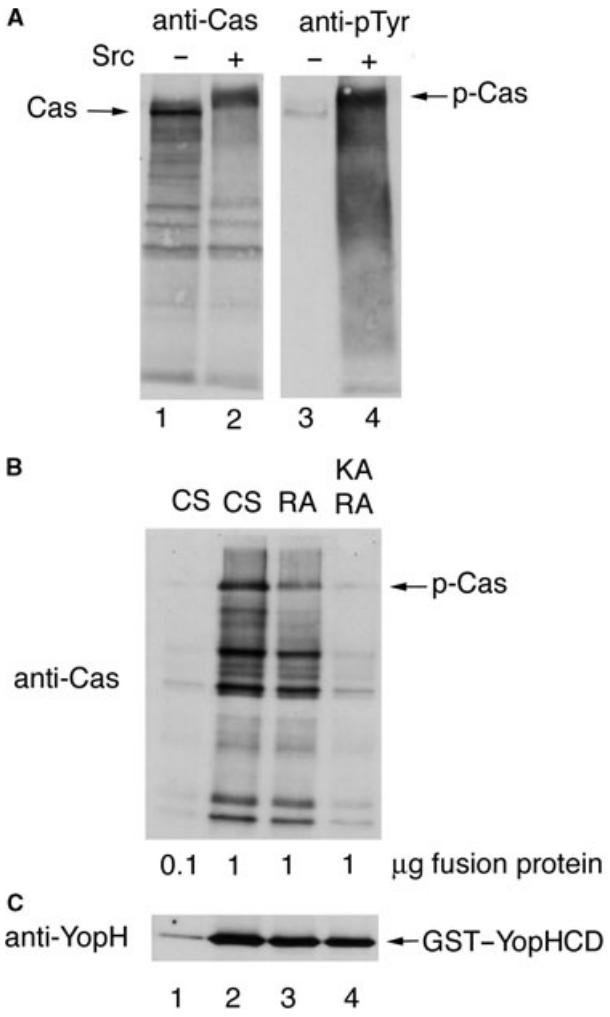

Fig. 4. The catalytic domain of YopH binds directly to tyrosine-phosphorylated Cas and site 2 is important for this activity.
A. Purified non-phosphorylated Cas protein (–Src) and Cas phosphorylated by v-Src kinase (+Src) were analysed by immunoblotting with anti-Cas or (lanes 1 and 2) anti-pTyr (lanes 3 and 4) antibodies. Positions of non-phosphorylated Cas and phosphorylated Cas (p-Cas) are indicated.
B. GST fusion proteins containing catalytic domains of mutant YopH proteins were immobilized on beads (0.1 or 1 μg input), incubated with p-Cas, and after washing, the amount of p-Cas bound to the GST fusion proteins was measured by anti-Cas immunoblotting. The GST fusion proteins contained the catalytic domains of $YopH^{C403S}$M45 (CS), $YopH^{R409A}$M45 (RA) or $YopH^{K342AR409A}$M45 (KARA).
C. Recovery of GST fusion proteins on the beads was measured by anti-YopH immunoblotting. The positions of bands corresponding to the GST–YopH catalytic domain (CD) proteins are indicated.

site 1 and the A site could simultaneously engage phosphotyrosine residues on the same Cas molecule. The model shown at the top of Fig. 3H illustrates a conformation in which sites 1 and 2 are engaged on a single Cas molecule, leaving the A site exposed to dephosphorylate an adjacent Cas molecule. It will be necessary to determine the structure of full-length YopH in complex with a model substrate to further elucidate the mechanism of substrate recognition.

Cas contains 15 phosphorylation sites with a consensus motif (D/E)(V/I)pY(D/Q)VPP, which contains the preferred consensus motif (pY)XXP for the SH2 domain of the Crk protein (Bouton *et al*., 2001). In this light, it is interesting to compare the mode of phosphopeptide binding to site 2 with phosphopeptide binding to Crk SH2 domain (PDB id 1JUF). In both structures, the phosphotyrosine moiety binds with its ring approximately parallel to the protein surface, located on loops between β-strands and near the N-terminus of an α-helix. In both cases an Arg and one or more serines are involved in ligating the phosphate moiety.

The EGFR-derived peptide used in this study does not contain the residues following the phosphotyrosine residues that are present in the p130Cas phosphorylation sites. Nevertheless, we speculate that a Cas-derived peptide would bind similarly. As the P+1 (Leu) side-chain in the present structure points towards Arg337, we propose that the Cas P+1 Asp would form an ionic interaction with that residue. The subsequent three hydrophobic residues V–P–P might bind in a relatively hydrophobic cleft between the α4-helix and three β-strands of the nearby β-sheet. Additional YopH–phosphopeptide complex structures will need to be solved to confirm this hypothesis.

Experimental procedures

Protein crystallography

The catalytic domain of YopH and $YopH^{C403S}$ (residues 163–468) from *Y. enterocolitica* were purified as described (Zhang *et al*., 1992). Both of these constructs contain the C235R mutation shown not to affect catalytic activity. The phosphotyrosine peptide acetyl-DADE(pY)L-NH_2 was synthesized at the University of Michigan Protein Core facility and the difluorophosphonomethyl-phenylalanine-containing peptide of the same sequence was kindly provided by Dr Robert Zamboni and Dr Michael Gresser, Merck Frosst, Montreal. $YopH^{C403S}$ (163–468) at a concentration of 10–12 mg ml^{-1} was pre-incubated with 1 mM of the pY-containing peptide and then mixed with an equal volume of precipitant containing 18–24% polyethylene glycol (PEG) 8000, 50–100 mM NaCl, 0.1% β-mercaptoethanol, 100 mM TrisCl, pH 8.5. Seeding of the rod-shaped crystals gave crystals as large as $0.8 \times 0.4 \times 0.4$ mm^3. Diffraction intensities were measured on an SDMS multiwire detector at room temperature and processed with MADNES (Messerschmidt and Pflugrath, 1987). Molecular replacement with the 1YTS structure was performed in X-PLOR, and the two protein complexes in the unit cell were refined with data to 3.0 Å resolution with crystallography and NMR system (CNS) (Brunger *et al*., 1998) with non-crystallographic symmetry restraints. To crystallize the complex with the difluorophosphonomethyl-phenylalanine-containing peptide, YopH (163–468) at 10 mg ml^{-1} in 1 mM imidazole, pH 7.5 was incubated with 0.5 mM peptide (final concentration) for 1 h at room temperature. Protein was

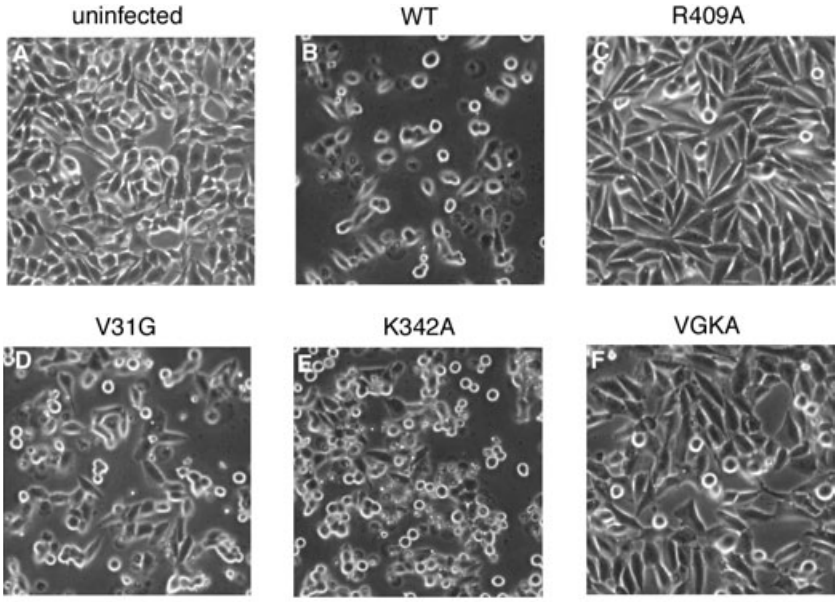

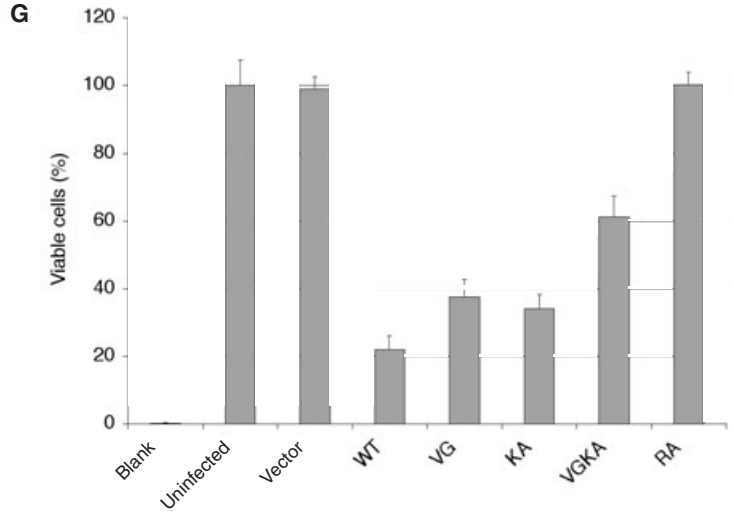

Fig. 5. Sites 1 and 2 co-operate to promote YopH cell detachment activity. HeLa cells were infected with *yopH* mutant *Y. pseudotuberculosis* strains for 1 h, bacteria were then killed by addition of gentamicin, and the cultures were incubated for an additional 18 h. Unbound cells were removed by washing.
A–F. Representative phase contrast images were captured by digital photomicroscopy.
G. Viable cells were quantified using an MTT assay. Results were normalized to uninfected cells. Results shown are the means and standard deviations of values obtained from three different wells for each condition performed in a single experiment and are representative of three independent experiments. The *yopH*^{VGKA} mutant promoted significantly less cell detachment than either the *yopH*^{VG} or the *yopH*^{KA} mutant ($P < 0.001$).

mixed with precipitant containing 22% PEG 4000, 8 mM $MnCl_2$, 0.1% β-mercaptoethanol, 100 mM Hepes, pH 7.5, and equilibrated by microvapour diffusion against the same precipitant. See Table 1 for data and refinement statistics. Co-ordinates are available from the Protein Data Bank (http://www.rcsb.org/pdb) as 1XXP and 1XXV.

Bacterial strains

The *Y. pseudotuberculosis* strains used for HeLa cell infection assays were derived from YP17 (*yopH::cam yopE::kan*) (Montagna *et al*., 2001). Plasmids derived from pMMB76HE which encode wild-type or mutant forms of YopH with appended M45 epitope tags (pPYopHM45, pPYopH^{R409A}M45, pPYopH^{V31G}M45 and pPYopH^{V31GR409A}M45) have been previously described (Montagna *et al*., 2001). Plasmids encoding additional mutant forms of YopHM45 (pPYopH^{K342A}M45, pPYopH^{K342AR409A}M45, pPYopH^{V31GK342AR409A}M45 and pPYopH$^{\Delta R409A}$M45) were constructed in the same vector using appropriate oligonucleotides and polymerase chain reactions. Plasmids were introduced into YP17 by conjugation (Montagna *et al*., 2001).

Yersinia pseudotuberculosis strains used in mouse infection studies were IP9 (*yopH::cam*), and additional *yopH* mutants derived from IP9 (Bliska *et al*., 1991). Mutant *yopH* alleles (*yopH*^{Nde}, *yopH*^{V31G}, *yopH*$^{\Delta 223–226}$, *yopH*^{K342A}, *yopH*^{R409A} and *yopH*^{VGKA}) were introduced onto the virulence plasmid carried by IP9 using the plasmid pSB890 and a standard allelic recombination strategy (Palmer *et al*., 1998). Following allelic recombination isolated colonies of *Y. pseudotuberculosis* were tested for loss of tetracycline resistance (to confirm excision of pSB890) and loss of chloramphenicol resistance (to confirm replacement of the *yopH::cam* allele). The presence of the virulence plasmid was verified by patching colonies on Congo red-magnesium oxalate agar plates (Riley and

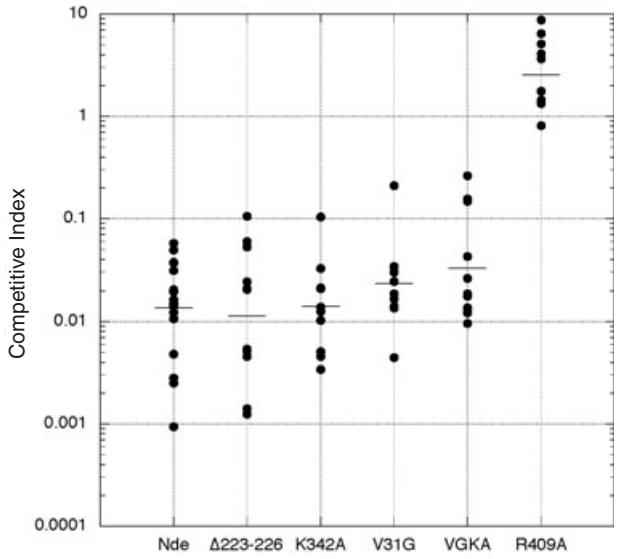

Fig. 6. Sites 1 and 2 co-operate to promote the virulence function of YopH in mice. Mice were infected intravenously with ≈500 cfu of a *Y. pseudotuberculosis* test strain (*yopH*^{Nde}, *yopHΔ223*$^{-226}$, *yopH*^{K342A}, *yopH*^{V31G}, *yopH*^{VGKA} or *yopH*^{R409A}) mixed with ≈500 cfu of the reference *yopH::cam* mutant. Four days post infection the mice were euthanized, the spleens were removed and homogenized, and dilutions of the homogenates were plated to enumerate output cfu of the reference strain (*cam*^{R}) and the test strain (*cam*^{S}). Competitive index (CI) values (filled circles) were transformed logarithmically to determine geometric means (horizontal bars) and *P*-values. The difference between the CI data for the *yopH*^{VGKA} competition and the *yopH*^{Nde} competition was statistically significant ($P = 0.044$).

Toma, 1989). Polymerase chain reaction was used to amplify the *yopH* sequences from prospective recombinants and the presence of the appropriate mutation was confirmed by sequencing. For infection assays, bacterial cultures were grown overnight at 28°C with shaking in Luria broth (LB), diluted in fresh media to an OD_{600} of 0.1 and grown with shaking at 37°C as described below.

In vitro *binding reaction*

Cas and v-Src were tagged at the N-terminus with polyhistidine and purified as described previously (Goldberg *et al*., 2003). *In vitro* kinase reactions with Cas and v-Src were performed as described previously (Goldberg *et al*., 2003). Plasmids that encode mutant forms of YopH catalytic domains fused to GST were constructed using pGEX-KG as described (Black *et al*., 2000). DNA fragments encoding residues 172–468 of the different mutant *yopH* alleles (*yopH*^{C403S}, *yopH*^{R409A} and *yopH*^{KARA}) with appended M45 tags were inserted between the *Sma*I and *Eco*RI sites of pGEX-KG. GST fusion proteins were expressed in *E. coli* TUNER cells (Novagen) and purified on GSTrap FF columns (Amersham Biosciences) using conditions suggested by the manufacturer. To start the binding reactions, 0.1 or 1 μg of purified GST fusion protein were diluted into 500 μl of binding buffer [phosphate-buffered saline (PBS)/1% BSA] and mixed with 20 μl of glutathione sepharose 4B (Amersham Biosciences). After 60 min incubation at room temperature, the beads were washed three times with binding buffer. Tyrosine-phosphorylated Cas (2.5 ng per reaction) was diluted into 500 μl of binding buffer containing 1 mM $NaVO_4$ and 10 mM NaF, and incubated with the beads pre-loaded with GST fusion protein. After incubation for 60 min at room temperature, the beads were washed twice with binding buffer containing 1 mM $NaVO_4$ and 10 mM NaF and twice with PBS containing 1 mM $NaVO_4$ and 10 mM NaF. The amount of Cas and GST fusion protein bound to the beads was measured by immunoblotting as described (Montagna *et al*., 2001).

HeLa cell infection

Yersinia pseudotuberculosis cultures were grow in LB containing 2.5 mM $CaCl_2$ and used to infect HeLa cells for immunoprecipitation, immunoblotting or immunofluorescence microscopy assays as described (Montagna *et al*., 2001). Immunoprecipitation, immunoblotting or immunofluorescence microscopy assays were performed as described (Montagna *et al*., 2001).

Yersinia pseudotuberculosis cultures used for MTT assays were grown in LB containing 20 mM $MgCl_2$ and 20 mM sodium oxalate for 1 h at 26°C and 2 h at 37°C. The cultures were washed with PBS and used to infect HeLa cells (1×10^5 per well in a 24-well tissue culture plate) at multiplicity of infection of 100. After 1 h of infection, the HeLa cells were washed once with PBS, and incubated in fresh medium containing 100 μg ml^{-1} gentamicin. At 19 h post infection detached cells were removed by washing with PBS and fresh media containing 500 μg ml^{-1} MTT (Sigma M-5655) was added to each well. After 4 h of incubation at 37°C/5% CO_2 the media was removed by aspiration and 100 μl of DMSO was added to each well. After 3 min incubation at room temperature, 900 μl of 0.04 N HCl-acidified isopropanol was added to each well and the plate was shaken thoroughly for 5 min. The absorbance of each sample at 570 nm was measured with a spectrophotometer (model ELx800, BIO-TEK Instruments). Values obtained from three different wells for each condition were averaged. Statistical significance was evaluated using one-way analysis of variance (ANOVA) and Tukey-Kramer Multiple Comparisons Test (Instat Version 2.01). A *P*-value of <0.05 was considered significant in individual comparisons.

Mouse infection

Yersinia pseudotuberculosis cultures for mouse infections were grown in LB for 3 h at 37°C. The cultures were washed in PBS and diluted to 10^4 colony-forming units (cfu) per millilitre. Each of the test strains was mixed with an equal volume of the reference strain (IP9, *yopH::cam*) and 100 μl of the mixture was injected into the tail vein of a 6- to 8-week-old female BALB/c mouse (Taconic). Input cfu (≈500 cfu of each strain, total of ≈1000 cfu) in each mixture was determined by plating on LB agar or LB agar containing chloramphenicol (30 μg ml^{-1}). Mice were euthanized 4 days post infection. Spleens were removed and homogenized in 4.5 ml of PBS. The total number of output cfu per spleen was determined by plating serial dilutions of the homogenates on LB agar. The number of output cfu corresponding to IP9 per spleen was determined by replica plating onto LB agar containing

chloramphenicol (30 μg ml^{-1}). CI values were calculated using the following formula:

(IP9 output cfu/test strain output cfu)/(IP9 input cfu/test strain input cfu)

Competitive index values were transformed logarithmically, and a two-tailed unpaired Student's *t*-test (InStat, version 2.01) was used to determine *P*-values, comparing the CI values from the IP9/*yopH*^{Nde} competition with CI values from other competitions.

Acknowledgements

We thank Patrick Hearing for providing M45 monoclonal antibody, and Lee Montagna for assisting with plasmid constructions. We also thank Parag Patwardhan and Todd Miller for generously providing purified Cas proteins, and Robert Zamboni and Michael Gresser for generous quantities of peptides. This work was funded by grants from the NIH awarded to J.B.B. (AI43389) and M.A.S. (AI34095) and from the American Cancer Society (J.A.S.).

References

Black, D.S., and Bliska, J.B. (1997) Identification of p130Cas as a substrate of *Yersinia* YopH (Yop51), a bacterial protein tyrosine phosphatase that translocates into mammalian cells and targets focal adhesions. *EMBO J* **16:** 2730–2744.

Black, D.S., Montagna, L.G., Zitzmann, S., and Bliska, J.B. (1998) Identification of an amino-terminal substrate-binding domain in the *Yersinia* tyrosine phosphatase that is required for efficient recognition of focal adhesion targets. *Mol Microbiol* **5:** 1263–1274.

Black, D.S., Marie-Cardine, A., Schraven, B., and Bliska, J.B. (2000) The *Yersinia* tyrosine phosphatase YopH targets a novel adhesion-regulated signalling complex in macrophages. *Cell Microbiol* **2:** 401–414.

Bliska, J.B. (2000) Yop effectors of *Yersinia* spp. and actin rearrangements. *Trends Microbiol* **8:** 205–208.

Bliska, J.B., Guan, K.L., Dixon, J.E., and Falkow, S. (1991) Tyrosine phosphate hydrolysis of host proteins by an essential *Yersinia* virulence determinant. *Proc Natl Acad Sci USA* **88:** 1187–1191.

Brunger, A.T., Adams, P.D., Clore, G.M., DeLano, W.L., Gros, P., Grosse-Kunstleve, R.W., *et al.* (1998) Crystallography & NMR system: a new software suite for macromolecular structure determination. *Acta Crystallogr D Biol Crystallogr* **54:** 905–921.

Bouton, A.H., Riggins, R.B., and Bruce-Staskal, P.J. (2001) Functions of the adapter protein Cas: signal convergence and the determination of cellular responses. *Oncogene* **20:** 6448–6458.

Carniel, E. (2002) Plasmids and pathogenicity islands of *Yersinia*. *Curr Top Microbiol Immunol* **264:** 89–108.

Carniel, E., Autenrieth, I.B., Cornelis, G., Fukushima, H., Guinet, F., Isberg, R., *et al.* (2002) *Y. enterocolitica and Y. pseudotuberculosis*. In *The Prokaryotes, an Evolving Electronic Resource for the Microbiological Community*, 3rd edn. Dworkin, M., Falkow, S., Rosenberg, E., Scheifer, K.H., and Stackebrandt, E. (eds). New York: Springer-Verlag.

Cornelis, G.R. (2002) The *Yersinia* Ysc-Yop 'type III' weaponry. *Nat Rev Mol Cell Biol* **3:** 742–752.

Deleuil, F., Mogemark, L., Francis, M.S., Wolf-Watz, H., and Fallman, M. (2003) Interaction between the *Yersinia* protein tyrosine phosphatase YopH and eukaryotic Cas/Fyb is an important virulence mechanism. *Cell Microbiol* **5:** 53–64.

Fällman, M., Persson, C., and Wolf-Watz, H. (1997) *Yersinia* proteins that target host cell signaling pathways. *J Clin Invest* **99:** 1153–1157.

Goldberg, G.S., Alexander, D.B., Pellicena, P., Zhang, Z.Y., Tsuda, H., and Miller, W.T. (2003) Src phosphorylates Cas on tyrosine 253 to promote migration of transformed cells. *J Biol Chem* **278:** 46533–46540.

Guan, K., and Dixon, J.E. (1990) Protein tyrosine phosphatase activity of an essential virulence determinant in *Yersinia*. *Science* **249:** 553–556.

Hueck, C.J. (1998) Type III protein secretion systems in bacterial pathogens of animals and plants. *Microbiol Mol Biol Rev* **62:** 379–433.

Khandelwal, P., Keliikuli, K., Smith, C.L., Saper, M.A., and Zuiderweg, E.R. (2002) Solution structure and phosphopeptide binding to the N-terminal domain of *Yersinia* YopH: comparison with a crystal structure. *Biochemistry* **41:** 11425–11437.

Mauro, L.J., and Dixon, J.E. (1994) 'Zip codes' direct intracellular protein tyrosine phosphatases to the correct cellular 'address'. *Trends Biol Sci* **19:** 151–155.

Messerschmidt, A., and Pflugrath, J.W. (1987) Crystal orientation and X-ray pattern prediction routines for area-detector diffractometer systems in macromolecular crystallography. *J Appl Cryst* **20:** 306–325.

Montagna, L.G., Ivanov, M.I., and Bliska, J.B. (2001) Identification of residues in the N-terminal domain of the *Yersinia* tyrosine phosphatase that are critical for substrate recognition. *J Biol Chem* **276:** 5005–5011.

Palmer, L.E., Hobbie, S., Galan, J.E., and Bliska, J.B. (1998) YopJ of *Yersinia pseudotuberculosis* is required for the inhibition of macrophage TNFα production and the down-regulation of the MAP kinases p38 and JNK. *Mol Microbiol* **27:** 953–965.

Perry, R.D., and Fetherston, J.D. (1997) *Yersinia pestis*-etiologic agent of plague. *Clin Microbiol Rev* **10:** 35–66.

Persson, C., Carballeira, N., Wolf-Watz, H., and Fallman, M. (1997) The PTPase YopH inhibits uptake of *Yersinia*, tyrosine phosphorylation of p130Cas and FAK, and the associated accumulation of these proteins in peripheral focal adhesions. *EMBO J* **16:** 2307–2318.

Persson, C., Nordfelth, R., Andersson, K., Forsberg, A., Wolf-Watz, H., and Fallman, M. (1999) Localization of the *Yersinia* PTPase to focal complexes is an important virulence mechanism. *Mol Microbiol* **33:** 828–838.

Phan, J., Lee, K., Cherry, S., Tropea, J.E., Burke, T.R., Jr, and Waugh, D.S. (2003) High-resolution structure of the *Yersinia pestis* protein tyrosine phosphatase YopH in complex with a phosphotyrosyl mimetic-containing hexapeptide. *Biochemistry* **42:** 13113–13121.

Ramamurthi, K.S., and Schneewind, O. (2002) Type III protein secretion in *Yersinia* species. *Annu Rev Cell Dev Biol* **18:** 107–133.

Revell, P.A., and Miller, V.L. (2001) *Yersinia* virulence: more than a plasmid. *FEMS Microbiol Lett* **205:** 159–164.

Riley, G., and Toma, S. (1989) Detection of pathogenic *Yersinia enterocolitica* by using congo red-magnesium oxalate agar medium. *J Clin Microbiol* **27:** 213–214.

Smith, C.L., Khandelwal, P., Keliikuli, K., Zuiderweg, E.R., and Saper, M.A. (2001) Structure of the type III secretion and substrate-binding domain of *Yersinia* YopH phosphatase. *Mol Microbiol* **42:** 967–979.

Stuckey, J.A., Schubert, H.L., Fauman, E.B., Zhang, Z.-Y., Dixon, J.E., and Saper, M.A. (1994) Crystal structure of *Yersinia* protein tyrosine phosphatase at 2.5A and the complex with tungstate. *Nature* **370:** 571–575.

Tonks, N.K., and Neel, B.G. (2001) Combinatorial control of the specificity of protein tyrosine phosphatases. *Curr Opin Cell Biol* **13:** 182–195.

Une, T., and Brubaker, R.R. (1984) *In vivo* comparison of avirulent Vwa$^-$ and Pgm$^-$ or Pstr phenotypes of *Yersiniae*. *Infect Immun* **43:** 895–900.

Zhang, Z.Y., Clemens, J.C., Schubert, H.L., Stuckey, J.A., Fischer, M.W.F., Hume, D.M., *et al.* (1992) Expression, purification and physiochemical characterization of a recombinant *Yersinia* tyrosine phosphatase. *J Biol Chem* **267:** 23759–23766.

Zhang, Z.-Y., Wang, Y., Wu, L., Fauman, E.B., Stuckey, J.A., Schubert, H.L., *et al.* (1994a) The Cys(X)5Arg catalytic motif in phosphodiester hydrolysis. *Biochem* **33:** 15266–15270.

Zhang, Z.-Y., Maclean, D., McNamara, D.J., Sawyer, T.K., and Dixon, J.E. (1994b) Protein tyrosine phosphatase substrate specificity: size and phosphotyrosine positioning requirements in peptide substrates. *Biochemistry* **33:** 2285–2290.